J Mater Sci (2007) 42:136–142
DOI 10.1007/s10853-006-1040-5

Studies on structural, dielectric and electrical properties of $Dy_xBi_{1-x}FeO_3$ solid solutions

V. L. Mathe · K. K. Patankar

Received: 25 September 2005 / Accepted: 4 January 2006 / Published online: 18 November 2006

Abstract The polycrystalline samples of $Dy_xBi_{1-x}FeO_3$ ($x = 1$, 0.8, 0.6, 0.4 and 0.2) were synthesized by standard solid state reaction technique. The samples synthesized were characterized by X-ray diffraction (XRD) technique. Further the samples were characterized by infrared (IR) spectroscopic technique. The dielectric measurements were carried out as a function of frequency in the range 100 Hz to 1 MHz at room temperature. Also the dielectric measurements were carried out as a function of temperature at certain fixed frequencies. The ac and dc resistivity measurements were carried out using two probe method. Also temperature dependence of ac and dc resistivity was noted. These measurements suggest polaron conduction in the samples. Finally, the data from XRD, IR, dielectric measurements were correlated.

Introduction

The interactions between various subsystems in the crystal formed an important branch of contemporary solid state physics. The investigation of electron–phonon, magnon–phonon, magnon–electron and other interactions as well as their influence on static and dynamic phenomena in crystal have led to discovery of several new effects. Magnetoelectrics, also known as seignetomagnetics (SMs), are of scientific interest. These materials exhibiting simultaneously long range electric and magnetic ordering stimulates an intense search for a new substance with similar properties. The interactions introduce number of peculiarities in ferroelectric and magnetic phase transition. These materials are of particular interest in the teaching, training and technology because they offer us an opportunity to learn from them in a unique way how nature is capable of combining elegantly in a single phase, but within the strict framework of symmetry rules, a whole palette of properties. Also they offer possibility to device single material platform that can support multi-functionality. The co-existence of electric and magnetic ordering, coupled within certain region of temperature and frequency are exploited as sensor, wave guide, modulator, switches, phase invertor, rectifier and find substantial application in radioelectronics, microwave electronics non-volatile random Access memory (NvRAM) [1, 2].

Bismuth ferrite ($BiFeO_3$) exhibits rhombohedrally distorted perovskite structure with space group R3c below ferroelectric transition temperature (T_{FE} = 1083 K) [3] and antiferromagnetic ordering up to 653 K (Neel temperature) [4]. At room temperature, it possesses both ferroelectric as well as antiferromagnetic ordering. Though the crystal symmetry of $BiFeO_3$ allows linear magnetoelectric (ME) effect but due to presence of cycloidal spin structure linear ME has not been observed in pure $BiFeO_3$ [5]. There are different possible contributions to the ME signal, such as electronic component, microscopic strains,

V. L. Mathe · K. K. Patankar
Department of Physics, Shivaji University,
Kolhapur 416 004, MS, India

Present Address:
V. L. Mathe (✉)
Department of Physics, University of Pune,
Pune 411 007, MS, India
e-mail: dearvikas_2000@yahoo.com

spin-orbital interactions, internal electrical and magnetic field, external field, etc [6]. The polarization is dependent on magnetic moment and electron momentum. Perusal of literature reveals that there are two ways to destroy cycloid spin structure present in pure $BiFeO_3$. One is by applying very high magnetic field of the order of 30 T [7]. Another way is substitution of Bi^{+3} (ionic radius = 1.20 Å) by rare earth element Dy (ionic radius = 0.99 Å). The substitution of rare earth in place of Bi seems to be producing observable, but weak magnetoelectric signal and enhanced dielectric properties. Our earlier work suggests that partial substitution of Bi^{+3} by rare earth elements of different ionic radius (such as La^{+3}, Nd^{+3}) enhances dielectric properties dramatically [8, 9]. Therefore to accomplish and realize the possibility of enhanced dielectric properties, we have prepared $Dy_xBi_{1-x}FeO_3$ solid solutions and studied their dielectric and electrical properties in detail.

Experimental

Polycrystalline samples of $Dy_xBi_{1-x}FeO_3$ with $x = 1$, 0.8, 0.6, 0.4 and 0.2 were prepared by standard solid state reaction technique. Oxides of Dy_2O_3, Bi_2O_3, and Fe_2O_3 were mixed together in required molar proportion and milled for 3 h. These samples were presintered at 1023 K for 12 h using programmable high temperature furnace, followed by grinding of an hour. The fine homogeneous powders were used to prepare pellets of diameter 10–15 mm and thickness of 3–4 mm by applying pressure of 5–6 tons using hydraulic press for 10–15 min. Two to three drops of saturated solution of polyvinyl alcohol (MW 14,000) were used as binder. Considering the difference in the melting point of initial ingredient the final sintering was carried out at different temperatures for different compositions under study so as to avoid melting of the samples and ensure the single phase formation of the samples. The optimized temperatures and sintering time are tabulated in Table 1. The single phase formation of the samples was confirmed by recording X-ray diffraction (XRD) patterns obtained by X-ray diffractometer (model PW 3710) using CuK_α radiation of wavelength 1.54056 Å). Further these samples were characterized by using IR spectrophotometer (Perkin Elmer model 783) in the frequency range 800–200 cm^{-1} to know stretching and bending vibration frequencies. The dielectric constant (ε') and dissipation factor (tan δ) measurements were carried out on all the samples as a function of frequency in the range 100 Hz to 1 MHz at room temperature using LCR bridge (model HP 4284A). Also the temperature dependence of ε' and tan δ were noted in the temperature range 300–750 K at certain fixed frequencies, viz. 1, 10, 100 and 1 MHz. The ac electrical resistivity measurements were carried out using LCR bridge (model HP 4284 A) at room temperature in the frequency range 100 Hz to 1 MHz and also as a function of temperature in the range 300–750 K at certain fixed frequencies namely 1, 10, 100 kHz and 1 MHz. The dc electrical resistivity measurements were carried out using two-probe method as a function of temperature in the range 300–750 K to understand aspect of electrical conduction in the present samples. Keithely electrometer (model 6514) was used for the current measurements. The detailed experimental procedures have been described elsewhere [10].

Results and discussion

Structural analyses

The XRD technique has been used for the structural analyses of the samples. The X-ray diffraction patterns for $Dy_xBi_{1-x}FeO_3$ with $x = 1$, 0.8, 0.6, 0.4 and 0.2 are shown in Fig. 1 (a–e) which suggest the single phase formation of the compounds. Few other peaks of intermediate phase in the XRD patterns have been observed for intermediate compositions. For example the peaks which comes in 25–30° of 2θ are of intermediate phase. Review of the literature on

Table 1 Crystal structure, lattice parameters and sintering temperature for $Dy_xBi_{1-x}FeO_3$

Composition	a (Å)	b (Å)	c (Å)	α (deg)	β (deg)	γ (deg)	Sintering temperature (K)		Crystal structure
							Pre-sintering for 12 h	Final sintering	
$DyFeO_3$	5.323	5.633	7.603	90.0	90.0	90.0	1023	1573 for 36 h	Orthorhombic
$Dy_{0.8}Bi_{0.2}FeO_3$	5.327	5.563	7.662	90.0	90.0	90.0	1023	1273 for 48 h	Orthorhombic
$Dy_{0.6}Bi_{0.4}FeO_3$	5.328	5.553	7.656	90.0	90.0	90.0	1023	1273 for 48 h	Orthorhombic
$Dy_{0.4}Bi_{0.6}FeO_3$	5.317	5.570	7.806	90.0	90.0	90.0	1023	1223 for 48 h	Orthorhombic
$Dy_{0.2}Bi_{0.8}FeO_3$	4.532	3.852	3.861	97.0	98.2	94.4	1023	1223 for 48 h	Triclinic

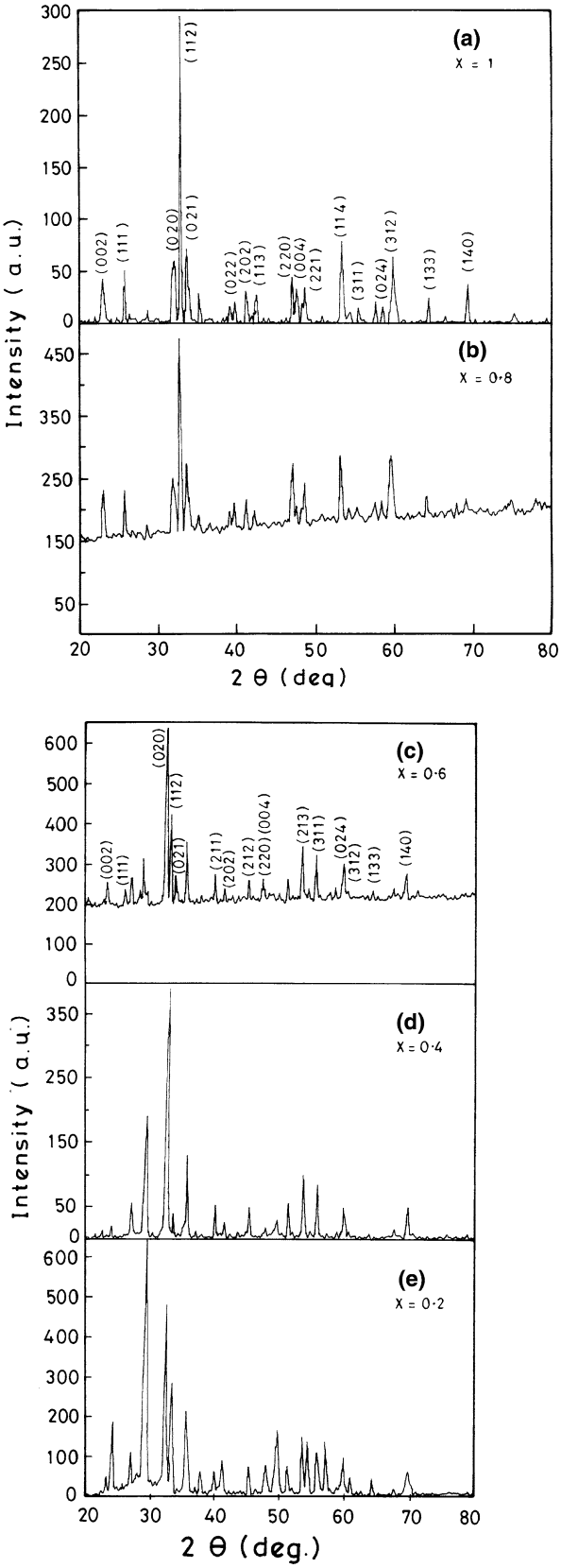

Fig. 1 (**a**–**e**) X ray diffraction patterns of $Dy_xBi_{1-x}FeO_3$ for $x = 1$, 0.8, 0.6, 0.4 and 0.2, respectively

$BiFeO_3$ (One of the end member of $Dy_xBi_{1-x}FeO_3$) and related materials speculates that the extra peaks observed are of $Bi_2Fe_4O_9$ [11–13]. Also comparison of observed '*d*' values with '*d*' values from JCPDS data of $Bi_2Fe_4O_9$ confirmed the speculation [14]. Synthesis of $Dy_xBi_{1-x}FeO_3$ solid solutions by solid state reaction technique revealed that formation of intermediate phase is unavoidable.

The samples prepared contain minimum extra phase. The analyses of the XRD patterns was carried out on the basis of polymorphism in $RE_xBi_{1-x}FeO_3$ (RE = rare earth) given by Murashov et al. [15] and JCPDS data of $DyFeO_3$ [16]. The analyses of the XRD data of the sample $x = 0.2$ was carried out by using computer software. The samples with $x = 1$, 0.8, 0.6 and 0.4 are orthorhombic and the sample with $x = 0.2$ is triclinic. The lattice parameters are calculated and tabulated in Table 1. The lattice parameters '*a*' and '*b*' remains fairly constant whereas the lattice parameter '*c*' goes on decreasing with increasing concentration of Dy^{+3}. This is due to lower ionic radius of Dy^{+3} as compared with Bi^{+3}. Such a variation of lattice parameters has been observed in cubic $Bi_xSr_{1-x}FeO_3$ system [17]. To understand cell volume variation with decrease in concentration of Dy, one has to consider polymorphism of $Dy_xBi_{1-x}FeO_3$ system and also the dependence of concentration boundaries on concentration of various rare earth elements (La^{+3}, Sm^{+3}, Nd^{+3}, Dy^{+3}, etc.) [15]. Careful evaluation of cell volume revealed that the cell volume goes on decreasing with decreasing x up to $x = 0.6$ and for $x = 0.4$ again it increases. The minimum observed at $x = 0.6$ which is rather corresponding to the half way mark of the maximum of entropy of mixing of solid solutions. The composition $x = 0.6$ lies at the boundary of polymorphic transition $C222_1$ to $Pna2_1$. Small symmetry changes from the crystallographic point of view might spell a dramatic change in terms of unit cell volume.

Infra red absorption studies

Infra red absorption spectra of a material give a good deal of information about Fe–O stretching and bending vibrations present in the samples. Subsequently, it helps us in correlating the dielectric data with change in crystal structure as a function of chemical composition. Figure 2 shows IR absorption spectra for $x = 0.6$ as a representative of others. The two absorption bands are observed in the measured frequency range. The absorption band at higher frequency (above 550 cm^{-1}) is labeled as ν_1 whereas the absorption at lower frequency (below 400 cm^{-1}) is labeled as ν_2. The

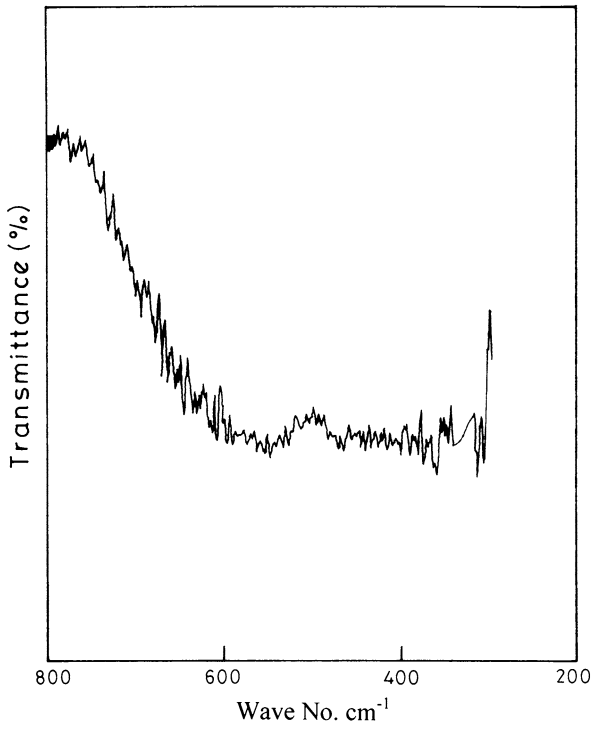

Fig. 2 IR absorption spectrum of $Dy_{0.6}Bi_{0.4}FeO_3$

absorption bands at v_1 are associated with Fe–O stretching normal vibrations while the absorption at v_2 are associated with Fe–O bending vibrations. Such absorption peaks have been observed for other orthoferrites [18]. From the absorption frequencies v_1 and v_2, the value of force constants K_s and K_b have been calculated using the standard procedure of solving secular equation [19]

$$\begin{vmatrix} (\mu_0+\mu_1)2k_s-\lambda_1 & \mu_0(4k_b) \\ -\mu_0(2k_s) & (\mu_0+\mu_1)4k_b-\lambda_2 \end{vmatrix} = 0 \qquad (1)$$

where μ_0 and μ_1 are the reciprocal masses of Fe and O ions, respectively, k_s and k_b are the force constant for stretching and bending vibrations, $\lambda = (2\pi v)^2$. The IR data for all the samples is tabulated in Table 2. It is observed that value of k_s and k_b is changing with change in Dy content. The inspection of absorption frequencies reveals that the broadness of the bands goes on increasing with change in crystal structure of $Dy_xBi_{1-x}FeO_3$ solid solutions. The sample with $x = 0.2$ shows more broader peaks in IR absorption whose crystal structure is triclinic and other samples of this family possess orthorhombic structure as revealed from XRD analysis. The absorption frequencies are sensitive to structure of $Dy_xBi_{1-x}FeO_3$ solid solutions rather than the mass of vibrating ions.

Dielectric studies

Figure 3 (a) shows variation of ε' versus frequency for $Dy_xBi_{1-x}FeO_3$ with $x = 1$, 0.8, 0.6, 0.4 and 0.2 at room temperature. The value of ε' is relatively higher at low frequencies. It shows small dispersion with increase in frequency up to 5 kHz and remains fairly constant afterwards. This is due to the fact that the dipoles are not following the frequency of applied field in the measured frequency range after 5 kHz. Figure 3 inset shows variation of ε' with change in Dy content. It is found that the sample with $x = 0.2$ possess higher dielectric constant amongst all the samples under study. It was our expectation to get enhanced value of ε' as compared to the end members of the series (i.e., $BiFeO_3$ and $DyFeO_3$) with substitution of Bi by Dy due to weakening of A–B sub lattice interactions. The change in dielectric constant is attributed to different competing interactions such as mismatch between A–O and Fe–O bands with different length compressibilities and thermal expansion, superexchange interactions in the ionic Fe–O bond versus double exchange interaction in metallic Fe–O bond. As observed in Table 2 the value of ε' varies in accordance with 'k_s', calculated from IR transmittance data for the samples having orthorhombic structure. Variation of dissipation factor 'tan δ' as a function of frequency at room temperature for all the samples under study is consistent with the ε' behavior of the corresponding samples. Typical room temperature values of tan δ at 10 kHz are given in Table 2.

Table 2 IR and electrical data of $Dy_xBi_{1-x}FeO_3$

Composition	v_1 (cm^{-1})	v_2 (cm^{-1})	$k_s \times 10^5$	$k_b \times 10^5$	ε' (RT) at 10 kHz	tan δ (RT) at 10 kHz	ΔE from resistivity (eV)
$DyFeO_3$	580	390	0.938	0.425	93.23	0.164	1.11
$Dy_{0.8}Bi_{0.2}FeO_3$	550	400	0.867	0.413	23.85	0.149	1.19
$Dy_{0.6}Bi_{0.4}FeO_3$	560	370	0.897	0.397	48.38	0.140	1.07
$Dy_{0.4}Bi_{0.6}FeO_3$	620	370	1.038	0.422	153.33	0.084	1.17
$Dy_{0.2}Bi_{0.8}FeO_3$	600	330	0.965	0.375	170.97	0.119	1.02

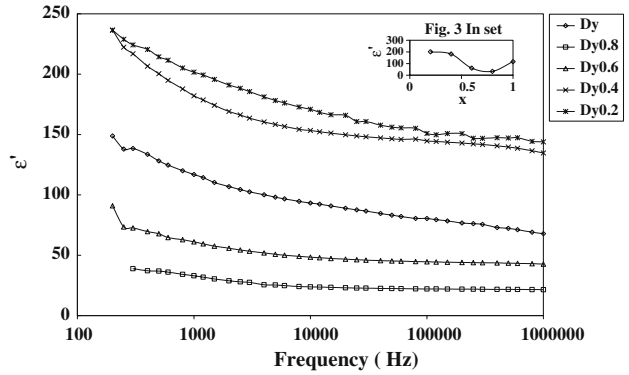

Fig. 3 Variation of ε' with frequency for $Dy_xBi_{1-x}FeO_3$ (x = 1, 0.8, 0.6, 0.4 and 0.2. (Inset) Variation of ε' with x for $Dy_xBi_{1-x}FeO_3$ at 12)

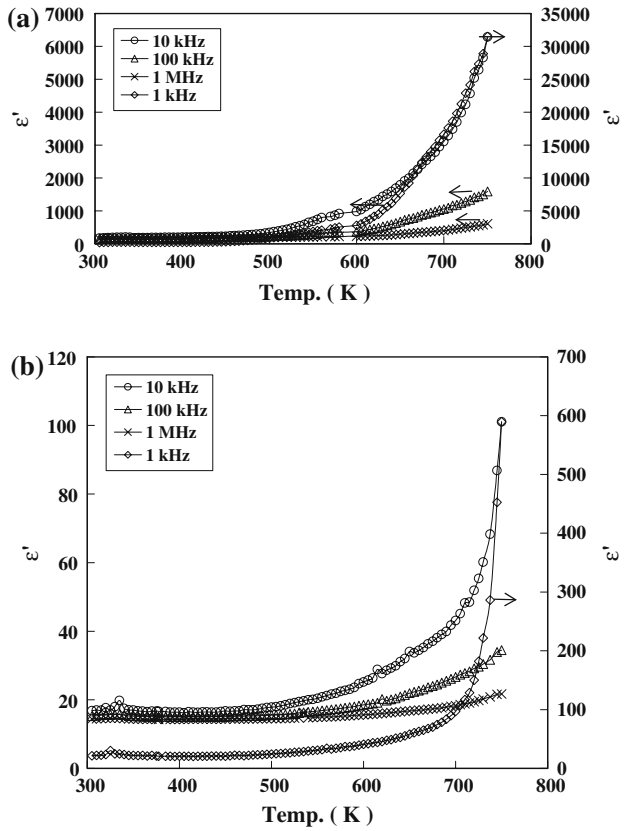

Fig. 4 (**a**–**b**) Variation of ε' with temperature at certain fixed frequencies namely 1, 10, 100 kHz and 1 MHz for x = 0.2 and x = 0.8, respectively

Figure 4 (a–b) shows the variation of ε' as a function of temperature in the range 300–750 K at certain fixed frequencies, viz., 1, 10, 100 kHz and 1 MHz for x = 0.2 and 0.8, respectively. The ε' remains fairly constant up to about 550 K, thereafter, it increases rapidly. The increasing trend in ε' is due to increased conductivity in this temperature region. All other samples show

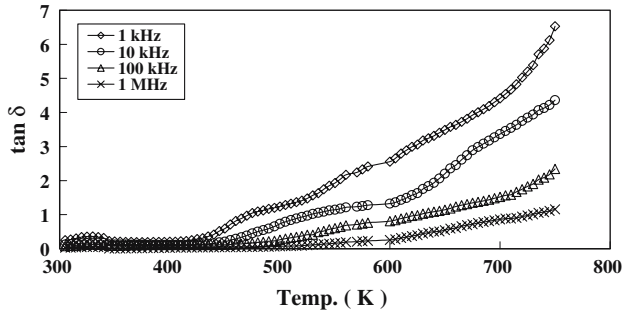

Fig. 5 Variation of tan δ with temperature at certain fixed frequencies namely 1 10, 100 kHz and 1 MHz for x = 0.2

similar trend of ε' with temperature. According to Krainik et al., for $BiFeO_3$ eight anomalies were observed in ε' versus temperature variation in the range 293–1123 K [20]. No such anomalies have been observed in the ε' measurements within the temperature range of measurement for $Dy_xBi_{1-x}FeO_3$ solid solutions. x = 0.2 sample exhibits relatively high value and x = 0.8 sample exhibits relatively low value even at higher temperature as observed at room temperature.

Figure 5 shows the variation of tan δ as a function of temperature in the range 300–750 K at certain fixed frequencies, namely 1, 10, 100 kHz and 1 MHz for x = 0.2. This shows small peak at around 325 K and remains fairly constant after words and show increasing trend above 500 K for all frequencies in the temperature range of measurement. The values of tan δ greater than 10 cannot be recorded by using LCR meter (model HP 4284 A) due to the meters limitation. The peak around 325 K is attribute to unknown transition which may be due to change of electric ordering from one state to another state. This is consistent with ε' behavior of the corresponding sample.

Resistivity studies

Figure 6 shows the variation of ln ρ (ac and dc) versus $1000/T$ for x = 0.2 (i.e., $Dy_{0.2}Bi_{0.8}FeO_3$). From these

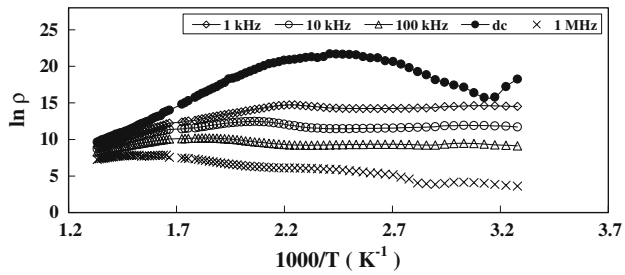

Fig. 6 Plot of ln ρ vs. $1000/T$ for $Dy_{0.2}Bi_{0.8}FeO_3$ (ac and dc variation of ρ)

plots, it is seen that the resistivity values changes in the range of the order of 10^8 Ω cm for dc to 10^2 Ω cm for 1 MHz frequency. This suggests polaron conduction by hopping mechanism. The trend of ac and dc electrical resistivity variation as a function of temperature is similar for other samples. At around 325 K, a cusp like minimum is observed for dc resistivity curve. At the same temperature small peak has been observed in tan δ measurements, which may be due to change of electrical ordering from one state to another. The resistivity values remain fairly constant up 450 K and decreases afterwards. This is consistent with ε' and tan δ variation as function of temperature. The activation energies are calculated in the linear region for all the samples. The value of activation energy is found to be greater than 0.2 eV, which is greater than the energy required for $Fe^{+2} \leftrightarrow Fe^{+3}$ transition. This suggests the conduction is due to polaron hopping. There is marked difference in ac and dc resistivity values at room temperature. This can be understood frequency dependence of polaron conduction by hopping mechanism. The excess electron in a narrow conduction band due to their interactions with ions distorts the surrounding in such a way that potential thereby generated is deep enough to introduce localization leading to the formation of polaron [21]. The small polaron conduction at higher temperature is frequency independent, which is indeed observed in resistivity measurements with temperature. At higher temperature, ac and dc resistivity values co-insides each other. This is due to the fact at room temperature there is contribution from defects, voids and impurities to the conduction while at higher temperature the conduction is intrinsic conduction. At room temperature conductivity σ $(1/\rho)$ depends upon the frequencies according to the relation [22]

$$(\sigma_{ac} - \sigma_{dc}) = (\omega^2\tau/(1 + \omega^2\tau^2) \quad (2)$$

where σ_{ac} is ac conductivity, σ_{dc} is dc conductivity, ω is the angular frequency, and τ is the relaxation time. From this relation, it is clear that hopping conduction of small polaron is completely unobservable in dc measurements. It is possible to observe the hopping of small polaron to impurity site as an additional contribution to ac conductivity. To get the idea of conduction mechanism, we measured σ as a function of frequency in the range 100 Hz to 1 MHz at room temperature for all the samples. Figure 7 shows the variation of log $(\sigma_{ac}–\sigma_{dc})$ vs. log ω^2 for x = 1, 0.8, 0.6, 0.4 and 0.2 samples. The nature of the graph is linear.

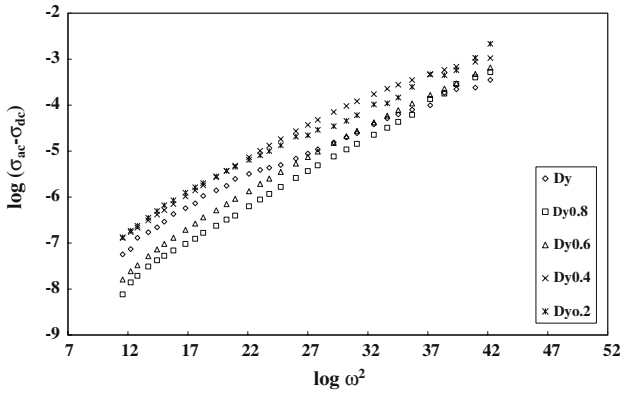

Fig. 7 Plot of log $(\sigma_{ac}–\sigma_{dc})$ vs. log ω^2 for $Dy_xBi_{1-x}FeO_3$ (x = 1, 0.8, 0.6, 0.4 and 0.2)

In such a case, σ_{ac} obeys the relation (2). Since τ is small (~10^{-6} s) at frequencies <1 MHz, $\omega^2\tau^2 << 1$ and hence it is neglected from the denominator of Eq. (2). Thus in such a case a plot of log $(\sigma_{ac} - \sigma_{dc})$ vs. log ω^2 should be straight line, which is indeed the case in Fig. 7. This confirms the polaron hopping conduction [10, 23].

Conclusions

The samples of $Dy_xBi_{1-x}FeO_3$ solid solutions were synthesised by solid state reaction method. The nature of the samples is polycrystalline. The crystal structures of $Dy_xBi_{1-x}FeO_3$ solid solutions are found to be orthorhombic for x = 1, 0.8, 0.6, and 0.4 and triclinic for x = 0.2. The IR spectrum suggests presence of stretching and bending vibrations. The force constant 'k_s' has been correlated with dielectric constant of the corresponding sample. The values of dielectric constant are higher for x = 0.2 as compared to the end members of the family $BiFeO_3$ and $DyFeO_3$. It is due to weakening of A–Fe sub lattice interactions. The activation energies are calculated from electrical resistivity measurement as a function of temperature suggests polaron hopping conduction. This is supported by dependence of conductivity on frequency at room temperature for all the samples.

Acknowledgements Authors are thankful to late Prof. SA Patil, who introduced us to the field of magnetoelectrics. Authors would like to acknowledge Prof. PB Joshi, Prof. RN Patil and Dr. CD Lokahande for the fruitful discussions. Authors (VLM & KKP) are thankful to CSIR, New Delhi for the award of SRF & Extd. SRF, respectively. Authors are thankful to referee for valuable suggestions.

References

1. de Araujo CAP, Mcmillan LD, Cuchiaro JD, Scott JF (1995) Nature 374:627
2. Mihara T, Yoshimori H, Watanable H, de Araujo CAP (1995) Jap J Appl Phys Part 1 34:5233
3. Popov Yu F, Kadomtseva AM, Vorob'ev GP, Zvezdin AK (1994) Ferroelectrics 162:135
4. Palkar VR, Pinto R (2002) Pramana 58:1003
5. Kadomtseva AM, Popov Yu F, Schogoleva TV, Vorob'ev GV, Zvezdin AK, Dubenko IS, Murashov VA, Rakov DN (1995) Ferroelectrics 169:85
6. Kornev I, Rivera JP, Gentil S, Jansen AGM, Bichurin M, Schmid H, Wyder P (1999) Physica B 271:304
7. Kadomtseva AM, Yu F Popov, Vorob'ev GP, Zvevdin AK (1995) Physica B 211:327
8. Mathe VL, Patankar KK, Kothale MB, Kulkarni SB, Joshi PB, Patil SA (2002) Pramana 58:1105
9. Mathe VL, Patankar KK, Patil RN, Lokhande CD (2004) J Mag Mag Mater 270:380
10. Mathe VL, Patankar KK, Lotke SD, Joshi PB, Patil SA (2002) Bull Mater Sci 25:347
11. Maheshkumar M, Srinath S, Kumar GS, Suryanarayana SV (1998) J Mag Mag Mater 188:203
12. Sosnowska I, Peterlin-Neumaier T, Steichele E (1982) J Phys C 15:4835
13. Jainding Yu, Naokiyo Koshikawa, Yasutomo Arai, Shinichi Yoda, Hirofumi Saitou (2001) J Cryst Growth 231:568
14. JCPDS Card No. 25–90
15. Murashov VA, Rakov DN, Ionov VM, Dubenko IS, Titov YU, Gorelik VS (1994) Ferroelectrics 162:11
16. JCPDS card No. 19–433
17. Li J, Duan Y, He H, Song D (2001) J Alloys Comp 315:259
18. Subba Rao GV, Rao CNR (1970) Appl Spectr 24:436
19. Kokare SR, Pawar SA, Padal NT, Joshi PB (2001) Bull Mater Sci 24:243
20. Krainik NN, Khuchua NP, Zhdanov VV, Euseev VA (1966) Sov Phys Solid Stare 8:654
21. Appel J (1968) Solid State Phys 21:193
22. Sirdeshmukh L, Krishn KK, Bal LS, Ramkrishna A, Sathaiah G (1998) Bull Mater Sci 21:129
23. Lal H, Dar N (1976) Ind J Pure Appl Phys 14:788